

## **Experimental observations and modeling of nanoparticles formation in laser-produced expanding plasma**

E. Lescoute<sup>1</sup>, L. Hallo<sup>1</sup>, D. Hébert<sup>2</sup>, B. Chimier<sup>1</sup>, V.-T. Tikhonchuk<sup>1</sup>, J.-M. Chevalier<sup>2</sup>

<sup>1</sup> *CELIA, Université Bordeaux I, France*

<sup>2</sup> *CEA-CESTA, Le Barp, France*

### **Introduction**

Interaction of a laser beam with a target produces a high velocity expanding plasma plume which can contain solid debris and liquid nano- and microparticles. A phenomenological model of vapor condensation described by Zel'dovich and Raizer (ZR) has been introduced in a 1D hydro-code and compared against experimental measurements of nuclei. Details and bibliography precisions can be found in [1]

### **Experimental results**

A laser system operating at 800 nm with the pulse duration varying from 40 to 165 fs has been used. The focal diameter was varied in the range 20 – 320  $\mu\text{m}$ , which enables a wide variation of laser fluences from 5 to 125  $\text{J}/\text{cm}^2$  conserving mainly a planar geometry, even though 2D effects are expected due to expansion of the plasma.

Gold targets were irradiated with a laser with  $\sim 125 \text{ J}/\text{cm}^2$  fluence. The collecting glass plates were located on the laser axis at the distance of 5 mm from the target. This regime corresponds to the curve 3 in Fig. 1 and we expected nano-particle formation. The deposited particles were analyzed with a photothermal detection microscope. Assuming spherical particle shapes, this diagnostic resolves the diameters in the range from 2 to a few tens nm (Fig. 2). A distribution of particles on sizes is presented in Fig. 3. The maximum diameter measured is about 50 – 60 nm, and the maximum number of particles is obtained at 9 nm.

### **Nucleation model**

The nanoparticles are formed when the corresponding vapor volume crosses the binodal, see Fig. 1, curve 3. Whereas droplet size and number are linked to the energy-mass balance, only the total amount of liquid, i.e. condensation degree, is obtainable from equilibrium considerations. However, plasma expansion is a very fast process, so the condensation proceeds in non-equilibrium conditions. The heterophase fluctuation theory by Frenkel supposes that nuclei of liquid phase are formed in inelastic atomic collisions.

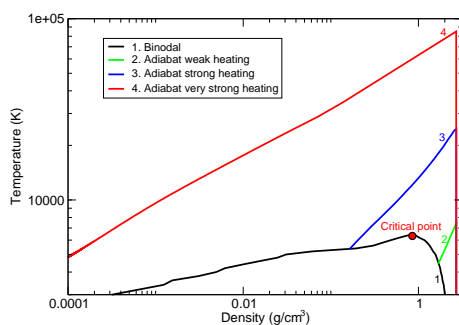


Figure 1: Temperature versus density thermodynamic diagram for aluminium. The binodal (1) limits the liquid-gas mixture domain from a gas (on the left from the critical point ) or from a liquid (on the right from the critical point). Curve 2 presents adiabatic expansion with droplets creation after a weak heating. Curve 3 presents adiabatic expansion with a partial recondensation after a strong heating. Curve 4 presents an adiabatic expansion with transition into the gas phase.

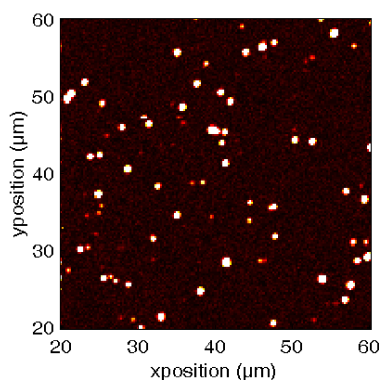


Figure 2: Substrate impacted by gold nano-particles. The incident laser fluence on the gold target is  $125 \text{ J/cm}^2$  and the substrate is located at 5 mm from the target. Image is obtained with a photothermal detection microscope.

### Nuclei growth and sticking

Neglecting the collisions between droplets and/or their coalescence, droplet evolution comes from a balance between the attachment of vapor atoms to the droplet surface and the evaporation of atoms from it. According to Frenkel and Raizer, a temperature equilibrium between the liquid droplet and the surrounding vapor can be assumed. In the plasma expansion issued from the laser energy release, the vapors are inhomogeneous, so the total number of droplets can be found by post-processing the density and temperature profiles and assuming the the total number of droplets is relatively small and does not affect the overall hydrodynamic evolution. The nucleation models provide the droplet size and number once the equilibrium temperature

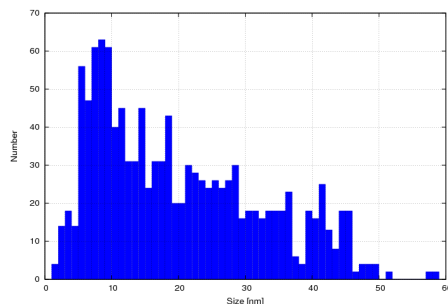


Figure 3: Distribution of particles on sizes obtained by the photothermal detection. The laser flux is  $125 \text{ J/cm}^2$  on a gold target.

is defined and the temperature evolution is computed from a hydrodynamic code.

### Numerical modeling

The experimental results presented above are compared with numerical simulations describing the hydrodynamic expansion of the target ejecta and its condensation according to the Frenkel-Raizer model. Modeling of the laser energy release and the target expansion is carried out with a one-dimensional (1D) hydrodynamic code ESTHER accounting for the laser energy release and non linear thermal transport with two temperatures for electrons and ions. Laser propagation and energy release are described by the Helmholtz equation.

With the code ESTHER we modeled the ablation process induced by a 165 fs,  $125 \text{ J/cm}^2$  laser pulse on a gold target. Distribution of particles on sizes obtained with the Frenkel-Raizer model for nuclei growth is presented in Fig. 4. It has to be compared to the experimental distribution presented in Fig. 3 for the same conditions. Both distributions have a similar shape. The model predicts the position of the maximum at the size of 2 nm and a sharp cutoff at 20 nm. The experimental distribution (Fig. 3) has a lower cutoff at larger diameters of 3 – 5 nm and the upper cutoff at the diameters of 50 – 60 nm. The lower cutoff in the experimental curve is defined by the resolution of the photothermal microscope. The two times difference between the model and experiment for maximum diameters can be explained by the coalescence of nuclei in air. This process is not taken into account in our model.

A number of simulations have been carried out in order to look to particle dimensions on laser fluence, for various laser pulse duration and wavelength. Results are presented in Fig. 5 for shots on aluminium and gold targets. It can be seen that nanoparticle size increases continuously with fluence. More precisely, nanoparticle diameters can be written

$$D \sim (\tau.I)^\alpha,$$

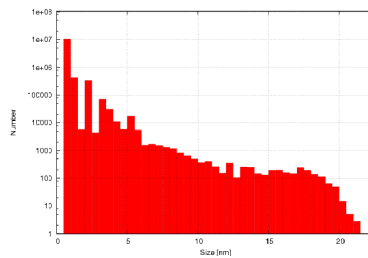


Figure 4: Distribution of nuclei on sizes obtained with the Frenkel-Raizer model for the  $125 \text{ J/cm}^2$  laser fluence at a gold target. The corresponding experimental data are presented in Fig. 2.

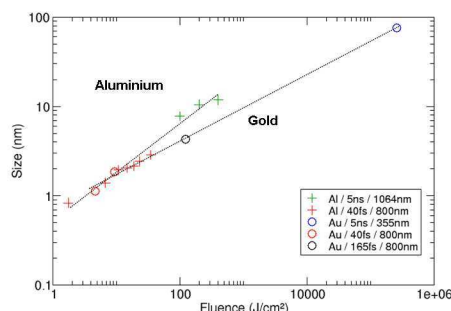


Figure 5: Size of nanoparticles on the laser fluence in aluminium and gold targets, for various laser wavelength, pulse duration.

where  $\alpha$  depends on the target material.

## Conclusion

Control of micrometric and submicrometric particle sizes and characteristics present a growing interest due to a recent interest to nanotechnology domain. Applications involved go from film deposition to optic adaptation. Particles of nanometric sizes can also be used in biology and chemistry. In the Laser Mega-Joule context, it is crucial to control the optical properties of the elements located in the experiment room, or simply to control the amount of metals which will have to be collected after several shots. We present some experimental results that we explain by a simple modeling.

## References

- [1] E. Lescoute et al, to be published, Phys. of Plasma, june 2008.